Supporting information

1. General

All reagents obtained from Sigma Aldrich or TCI or SRL Chemicals used without further modification, including spectroscopic grade solvents like Dioxane. HiMedia Chemicals, Mumbai, India, supplied Roswell Park Memorial Institute (RPMI 1640), Dulbecco's Modified Eagle Medium (DMEM), Dimethyl sulfoxide (DMSO), Phosphate buffer with a pH of 7.0, trypsin−EDTA, and U.S.-origin fetal bovine serum (FBS). Syringe filters (0.2 μM) were sourced from Sartorius, Ireland. Additional chemicals, such as Dichlorodihydrofluorescein diacetate DCFDA, 4′,6-diamidino2-phenylindole (DAPI), and Propidium iodide (PI), were purchased from Sigma Aldrich. Deionized water (18 MΩ) was produced using a Milli-Q synthesis system (Millipore, Billerica, MA). Analytical techniques involved recording ^{1}H NMR spectra on Bruker 600 MHz spectrometer, and ^{13}C NMR on 150 MHz spectrometer, with chemical shifts (δ in ppm) determined by fixing the solvent peak position. MALDI-TOF was performed on Bruker daltonics Autoflex Speed. MALDI TOF System (GT0263G201) spectrometer using matrix of trans-2-[3-(4-tert-Butylphenyl)-2-methyl-2-propenylidene] malononitrile (DCTB). FT-IR spectra were obtained with a JASCO model FTIR-4600. Melting points were measured with the Tempo and Mettler FP1 melting point instrument. Electronic absorption spectra and fluorescence spectra were recorded with a JASCO model V-770 UV-VIS-NIR Spectrophotometer and FP-8300 spectrometer, respectively. Morphological evaluations were conducted through transmission electron microscopy (TEM) using copper grids (JEOL 2100, 200 kV, USA) at an accelerating voltage of 200 kV under vacuum. FE-SEM measurements were performed on a JEOL JIB4700F (FIB-SEM), where all samples were deposited on a Si substrate by Spin coating and dried under vacuum at room temperature. DLS was measured using Zeta Potential Analyser, Nicomp Nano Z3000.

2. Synthesis and characterization

Eh-PDI[1] was synthesized according to the literature methods.

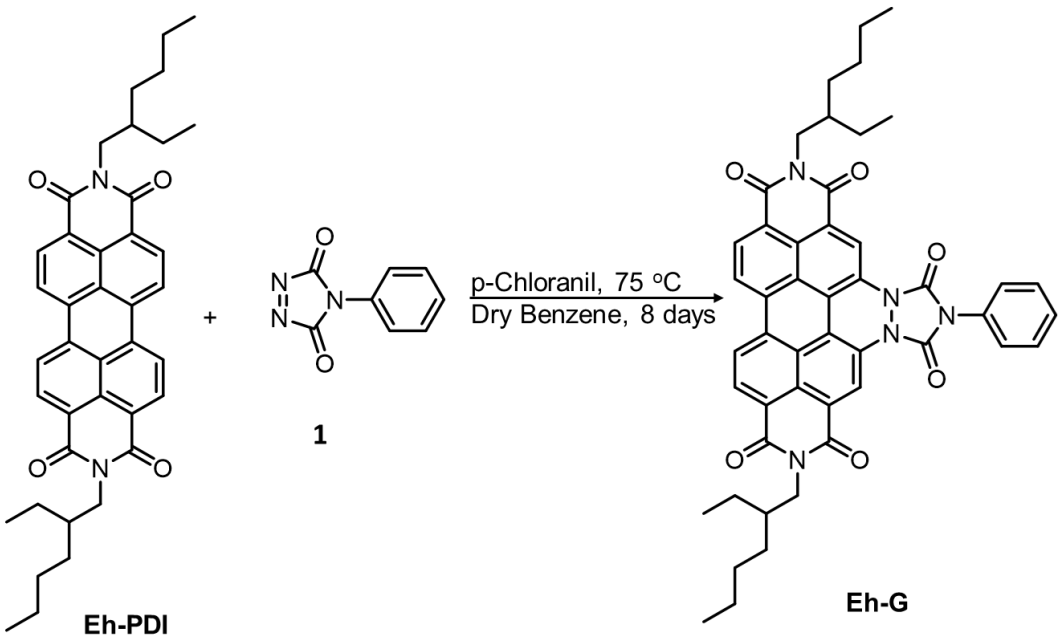

Scheme 1 Synthesis of **Eh-G**

In a 25 mL round bottom flask, a solution of **Eh-PDI**, (1 eq, 0.63 mmol, 0.500 g) in dried benzene (5 mL) was prepared. To this solution, 4-Phenyl-1,2,4-triazolin-3,5-dione,1, (5 eq, 3.17 mmol, 0.561 g) and *p*-Chloranil, 3 (2.5 eq, 1.585 mmol, 0.396 g), were added. The mixture was degassed with nitrogen gas for 30 minutes. Subsequently, the reaction mixture was heated at 75 °C for a duration of 7 days under continuous stirring, maintaining inert conditions. TLC was employed to monitor the progress of the reaction. After 7 days, the reaction mixture was cooled to room temperature, resulting in the formation of a precipitate. The precipitate was filtered, washed with hexane, followed by acetone, and the resulting solid was dried under reduced pressure. The crude product was purified using silica gel with a chloroform and acetone elution system, yielding a green solid, **Eh-G** at 1% acetone in chloroform. The obtained yield was 75%. ^{1}H NMR (400 MHz, $CDCl_3$) δ 8.90 (s, 2H), 8.01 (d, J = 7.9 Hz, 2H), 7.83 (d, J = 8.1 Hz, 2H), 7.61 (d, J = 7.5 Hz, 2H), 7.57 – 7.42 (m, 3H), 3.87 (m, 4H), 1.79 (t, J = 12.0 Hz, 2H), 1.37 – 1.16 (m, 16H), 0.84 (t, J = 11.4 Hz, 12H). ^{13}C NMR (150 MHz, $CDCl_3$) δ 162.10, 161.43, 142.91, 132.91, 132.20, 130.48, 129.80, 129.37, 126.06, 125.77, 124.74, 123.33, 123.12, 117.83, 116.07, 44.30, 37.83, 30.59, 28.56, 23.88, 23.07, 14.17, 10.47. IR (KBr): ~=344.03 cm-1 (w), 2940.91 (w), 1758 (m), 1700.91 (s), 1725. 98 (m), 1660.41 (s), 1500.13 (w), 1303.64 (m), 744.38 (m). MS: MALDI-TOF. Calculated 787.072 Found: 787.073.

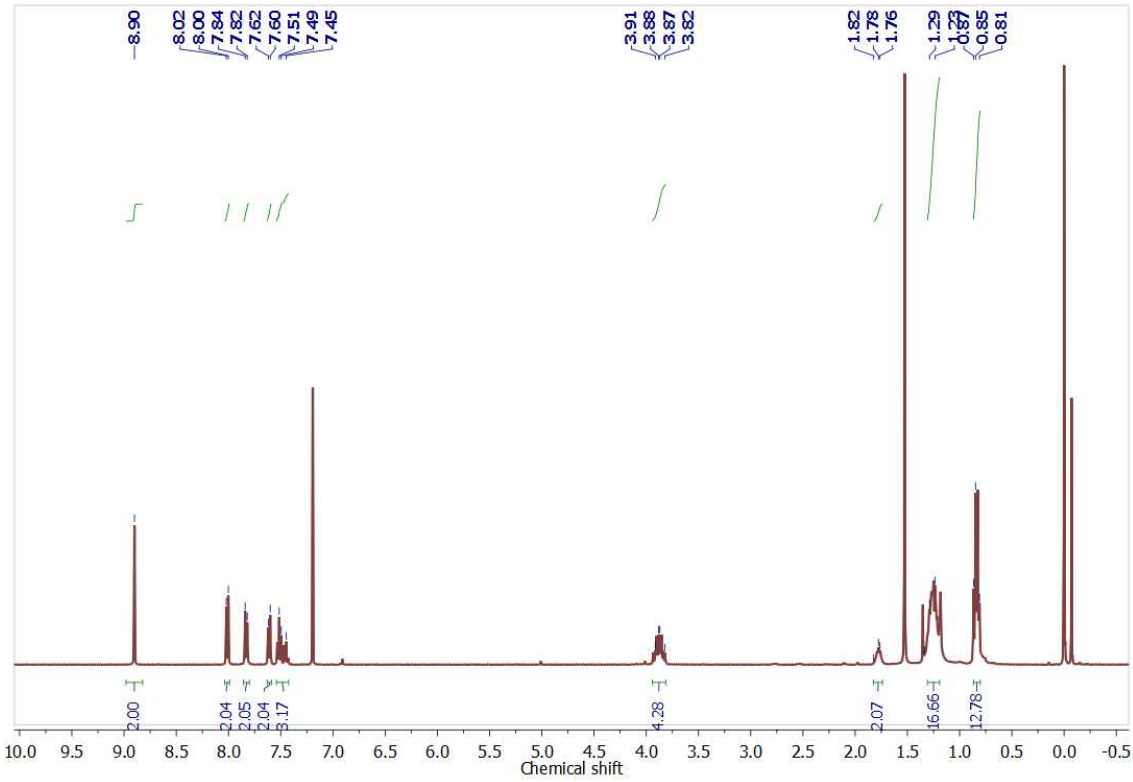

Figure S1. ^{1}H NMR spectrum of **Eh-G**.

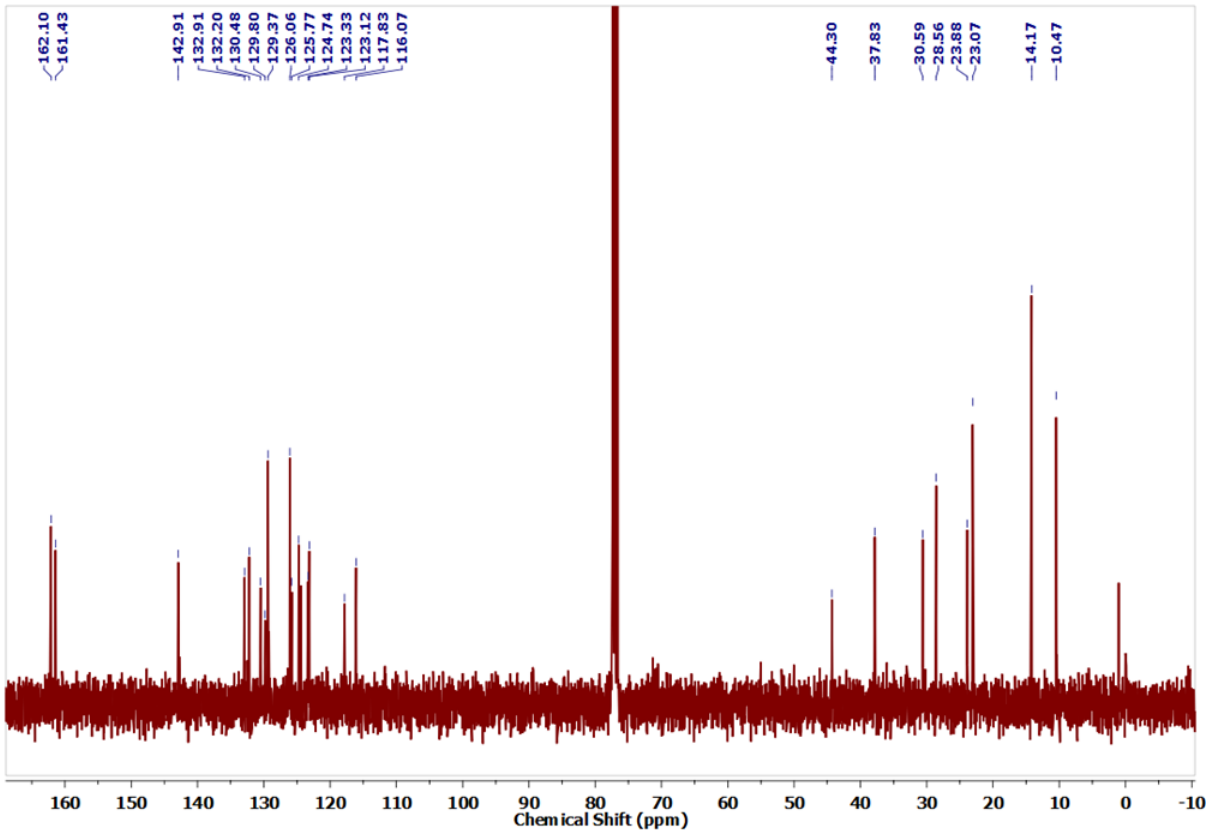

Figure S2. ^{13}C NMR spectrum of **Eh-G**.

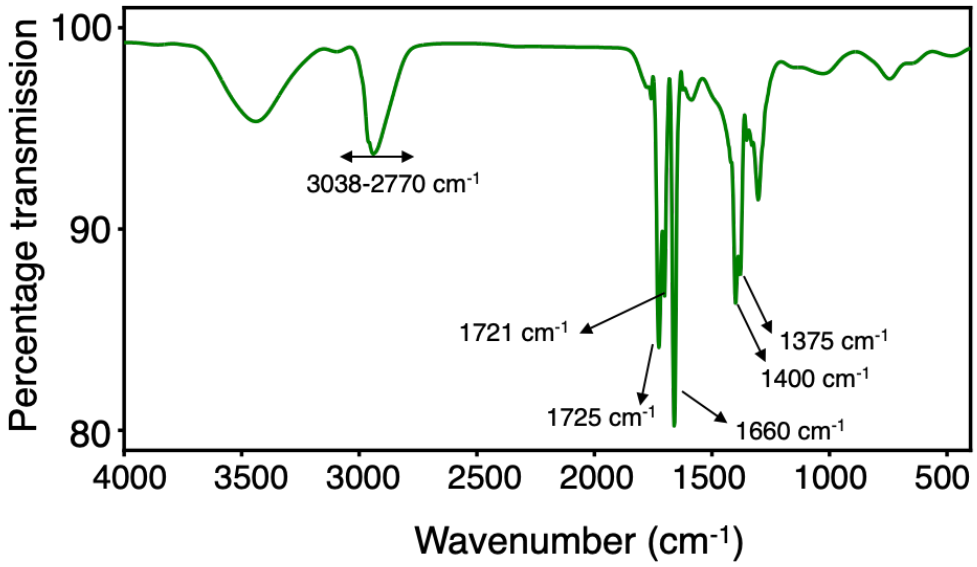

Figure S3. FTIR spectrum of **Eh-G**. 3038-2770 cm^{-1} (aromatic and aliphatic C-H stretching), 1725 cm^{-1}, 1721.98 cm^{-1} (symmetric and asymmetric carbonyl groups), 1660 cm^{-1} (aromatic C=C stretching), 1400 &1375 cm^{-1}(C-N stretching).

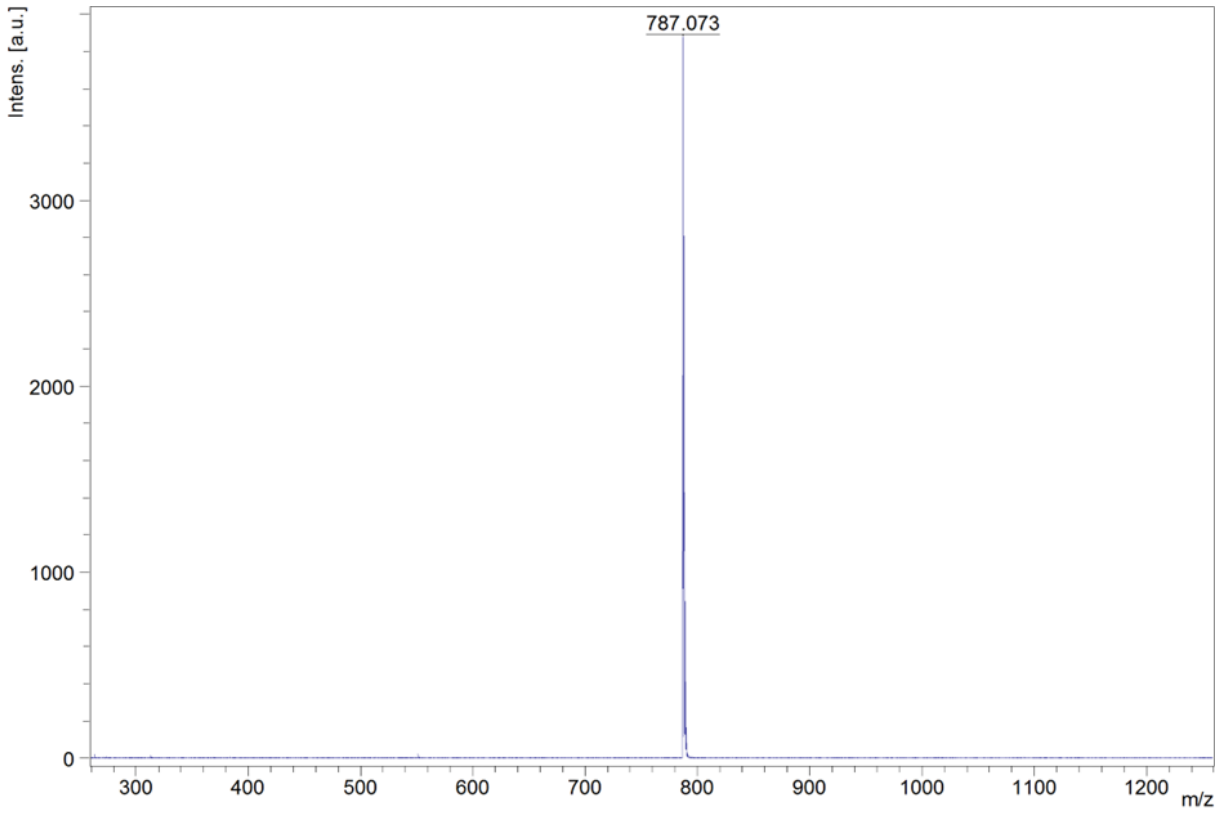

Figure S4. MALDI-TOF spectrum of **Eh-G**

3. Materials and methods

3.1. Cell Lines and Maintenance-

The human triple-negative breast cancer cell line 4T1, the mouse embryonic fibroblast L929, and the mouse embryonic fibroblast cell line NIH 3T3 were provided by the National Center for Cell Science (NCCS), Pune, India, for the purpose of this study. The L929 cell lines were cultured in DMEM media, while the 4T1 cell lines were cultured in RPMI medium supplemented with 10% (v/v) FBS, 1% L-glutamine, and 100 U/mL streptomycin/penicillin. Both cell types were maintained at 37 °C in a humidified environment with 5% CO_2.

3.2. Preparation of liposomal coated Eh-G nanoformulations-

As per Rengan et al. [2] the formulation of liposome-coated **Eh-G** nanoformulations (**L-Eh-G**) involved the thin film hydration technique. In brief, a mixture of 20 mg of soya pc was dissolved in 3 mL of chloroform/methanol (2:1). The resulting solution was subjected to rotary evaporation at 40 °C for 30 minutes to create a thin film. Subsequently, the film was hydrated for one hour at 60 °C with an appropriate quantity of milli-Q water. Following a similar procedure, liposomes loaded with the **Eh-G** compound were produced by dissolving 1 mg of each chemical separately in the organic phase. UV spectroscopy was employed to determine the amount of entrapped Eh-G. To remove bound chemicals, a 100 µL aliquot of the stock was collected and centrifuged at 10,000 rpm for 10 minutes. The absorbance of the pellet, dissolved in methanol, was measured using a UV-visible spectrophotometer. The absorbance was extrapolated using uncoated **Eh-G** standard curves. Each experiment was conducted in triplicate. The entrapment efficiency (EE) was calculated using the following equation:

$$\text{EE (\%)} = \frac{\text{Eh-G compound present in the nanoformulation}}{\text{Total compound}} \text{X } 100$$

3.3. Characterization of L-Eh-G nanoformulations-

The liposomal coated **Eh-G** compound (**L-Eh-G**) was characterized by UV–vis spectroscopy (Shimadzu UV-1800, Japan). The hydrodynamic diameter of prepared nanoformulations was analyzed by dynamic light scattering (Zeta Potential Analyser, Nicomp Nano Z3000)

3.4. Photothermal transduction efficacy

To assess the photothermal transduction efficiency of the **Eh-G** compound, different wells in 96-well plates, with or without liposomal coating, were treated with these compounds at a concentration of 20 µM. A 750 nm NIR laser with a power source of 650 mW (Shanghai Inter-Diff Optoelectronics Technology Ltd.) was employed to irradiate the wells for 0, 3, 5, 7, and 10 minutes. For photothermal transduction efficiency using 808 nm laser, power used was 808 mW. Deionized water and free liposomes served as controls. A thermal imaging camera (CHAUVIN ARNOUX, CA 1950 DiaCAm IR CAMERA IP 54 Paris, France) recorded temperatures and images at various time points. The photothermal stability of the **Eh-G** compound, with and without liposomal coating, was further assessed through NIR laser-mediated ON/OFF cycles (5 cycles) at 10-minute intervals.[2]

4. *In-vitro* studies

4.1 Biocompatibility studies

Biocompatibility experiments utilized L929 and NIH 3T3 cell lines to assess the biocompatibility of the **Eh-G** compound. The MTT (3-(4,5-Dimethylthiazol-2-yl)-2,5-diphenyl tetrazolium bromide) test was employed at concentrations of 10, 20, 40, 60, 80, and 100 M. A growth medium of DMEM (100 µL/well) was used, and 7×10^7 cells/wells were seeded in various 96-well plates. After 24 hours of incubation, fresh media containing **Eh-G** and **L-Eh-G** compounds were added to the DMEM medium. The treated cell plate was then placed in a CO2 incubator. The following day, 100 µL of MTT solution (5 mg/mL) was added

to each well and incubated for 3 hours. Subsequently, formazan crystals were gently dissolved by adding DMSO, and the absorbance was measured at 570 nm and 630 nm using the BIORAD Microplate Reader [3].

4.2 Cytotoxic activity

The cytotoxicity of **Eh-G** in 4T1 cell lines was examined using the MTT assay technique. Four 96-well plates were used, with RPMI serving as the growth medium (100 µL/well), and 4T1 cells were seeded at a density of 7×10^3 cells/well. After 24 hours, the RPMI media were replaced with media containing 20 µM of **Eh-G** and **L-Eh-G**, followed by irradiation with a NIR 750 nm laser (650 mW) or 808 nm laser (808mW) for 5 minutes per well. Following irradiation, the plates with cells were placed in a CO_2 incubator for a 6-hour incubation period. MTT solution (5 mg/mL) was then added, and the cells were further incubated for 3 hours. The formazan crystals were dissolved by adding DMSO, and for quantification, the absorbance of the dissolved formazan crystals was measured at 750 nm using a microplate reader (BIORAD Microplate Reader)[2]. Similar experiments were performed for 808 (808mW) laser.

4.3 In-vitro Live/Dead imaging for cell viability of 4T1 cancer cells

The cytotoxicity of **L-Eh-G** was qualitatively assessed using a live-dead assay on 4T1 cells. In 96-well plates, 4T1 cells (6×10^3) were seeded with RPMI as the growth medium (100 µL/well). After 24 hours, the RPMI media were replaced with media containing 20 µM of a free **Eh-G** compound and 20 µM of the **Eh-G** compound that had been liposomally coated, followed by exposure to a 5-minute NIR 750 nm laser treatment (650 mW) or 808 nm (808mW). FDA-PI staining (1 µM) was then performed, and the cells were incubated at 37 °C for 5 minutes. Fluorescence images were captured using an Olympus fluorescence microscope[2]. Same experiment was performed for 808 nm(808mW) laser.

4.4 Intracellular uptake studies in 4T1 cells

5×10^5 4T1 cells were seeded on the circular coverslip and put in a 12-well plate for intracellular uptake tests. Cells were treated with 20 µM of free Nile red, free **Eh-G**, compound, **L-Eh-G** incubated for 6 hours before being washed in PBS. This was done after the cells had been incubated for 24 hours. After being fixed with 4% paraformaldehyde followed by 1XPBS wash, the cells were stained with DAPI and MitoGreen. Images were captured using ZOE^{TM} Fluorescent Cell Imager[3].

4.5 ROS generation assay using DCFDA assay.

After a 24-hour incubation period, 4T1 cells (7×10^3) were treated with **Eh-G** and **L-Eh-G** at a concentration of 20 µM. Subsequently, 10 µM DCFDA was added, and absorbance measurements were taken on a fluorescence multimode plate reader both before and after 5 minutes of NIR laser irradiation with a 750 nm laser (650 mW) and 808 nm (808 mW). The excitation wavelength (Ex.) used was 485 nm, and the emission wavelength (Em) was set at 535 nm. Corresponding images were captured using an Olympus fluorescence microscope[3].

4.6 Singlet oxygen species analysis using SOS G.

The intracellular singlet oxygen ($^1O_2$) production efficiency of **L-Eh-G** was assessed before and after NIR laser irradiation using Singlet Oxygen Sensor Green (SOS G). 4T1 cells (7×10^3/wells) were seeded in 96-well plates and incubated for 24 hours in a CO_2 incubator. The following day, cells were incubated with probe-free liposomes, 20 µM of **Eh-G**, and **L-Eh-G**. Subsequently, cells were irradiated with a 750 nm NIR laser (650 mW) and 808 nm laser

(808 mW), and SOS G was introduced to the cells. Fluorescence was measured immediately before and after irradiation using a fluorescence microplate reader with Ex: 504 nm and Em: 525 nm wavelengths. Images were also captured using an Olympus fluorescence microscope[4,5].

4.7 3D breast cancer model for mimicking the in-vivo tumor microenvironment

4T1 cells (7×10^3/wells) were seeded in 96-well plates coated with 1% agarose. The plates were then placed in a CO_2 incubator and left undisturbed for 4 days to allow the formation of spheroids. After 4 days, the spheroids were transferred to new 96-well plates and treated with probe-free liposomes, 20 μM of **Eh-G**, and **L-Eh-G**. Subsequently, the spheroids were irradiated with a 750 nm laser (650 mW) and incubated for an additional 6 hours. The spheroids were then stained with FDA/PI to observe live and dead cells using a fluorescence microscope[6,7].

4.8 Photothermal efficiency

NIR photothermal heating was achieved by irradiating materials with a 750 nm laser for 20 minutes and 808 nm laser for 10 minutes. A thermocouple was attached to the vial's side to measure the temperature. The photothermal transduction efficiency (η) was estimated using previously described formulae.[8]

$$\eta = \frac{hS(T_{max} - T_{surrounding}) - Q_{dis}}{I(1-10^{-A750})} \quad (1)$$

Where h is the heat transfer coefficient, S is the surface area of the vial, T is the solution temperature, T_{Surr} is the temperature of the surrounding, T_{max} is the maximum steady-state temperature of the sample solution, Q_{dis} = is the heat dissipated from the light absorbed by the water and container, I is incident laser power, and A750 is the absorbance of **L-Eh-G** at 750 nm.

To find Q_{dis} same experiment was conducted with water as control

$$Q_{dis} = hS\,(T_{max} - T_{surrounding})_{water} \quad (2)$$

The term hS was calculated based on –

$$hS = \frac{mC_p}{\tau_s} \quad (3)$$

where, τ_s is sample system time constant, m is mass, C_p is the heat capacity (4.2 J $g^{-1}{}^{o}C^{-1}$) of water.

τ_s is related to a dimensionless driving force temperature θ by

$$t = -\tau_s \ln(\theta) \quad (4)$$

Where t is cooling time and θ is dimensionless temperature

$$\theta = (T - T_{surr})/(T_{max} - T_{surr})$$

The τ_s was determined by plotting the time versus negative logarithm of θ.

The Cooling time as a function of −ln(θ) is given for water, and samples are given in Figure S9.

For 750 nm laser irradiation: The τ_s is the slope of the graph, for water τ_s is 177.98 s. Thus, with the help of equation (3), hS was deduced to be 2.36 mW/°C after taking m = 0.1 g and C = 4.2 J g^{-1} $°C^{-1}$. The T_{Surr} and T_{Max} of water are 16.3°C and 25.5 °C, respectively. The Q_{Dis} is 21.71 mW, calculated based on equation (2). Similarly, the τ_s for the sample is 243 s. The hS is 1.73 mW/°C. The T_{Surr} and T_{Max} of the sample is 25 °C and 75.5 °C, respectively. I was 650 mW, and A750 was determined to be 0.116 at 750 nm. Substituting the obtained values in equation (1), the photothermal transduction efficiency (η) of **L-Eh-G** is 42.9%.

For 808 nm laser irradiation: The τ_s is the slope of the graph, for water τ_s is 143.6 s. Thus, with the help of equation (3), hS was deduced to be 2.92 mW/°C after taking m = 0.1 g and

C = 4.2 J g^{-1} $°C^{-1}$. The T_{Surr} and T_{Max} of water are 16.3°C and 23.4 °C, respectively. The Q_{Dis} is 20.17 mW, calculated based on equation (2). Similarly, the τ_s for the sample is 166 s. The hS is 2.53 mW/°C. The T_{Surr} and T_{Max} of the sample is 16.5 °C and 47.6 °C, respectively. I was 808 mW, and A808 was determined to be 0.08 at 808 nm. Substituting the obtained values in equation (1), the photothermal transduction efficiency (η) of **L-Eh-G** is 43.0%.

4.9 Statistical analysis

One-way ANOVA test was used to compare the control and the treated groups. Tukey's test was used for comparison among groups ($*p<0.05$, $**p<0.01$,$***p<0.001$).

4.11 Stability of L-Eh-G in media

For the measurement of stability of L-Eh-G in serum containing media we employed the use of RPMI media. The media was mixed with **L-Eh-G** and its UV-Vis-NIR spectrum was monitored for 6 days to analyse any degradation or changes in peaks indicating degradation of **L-Eh-G.**

5. Supporting Figures

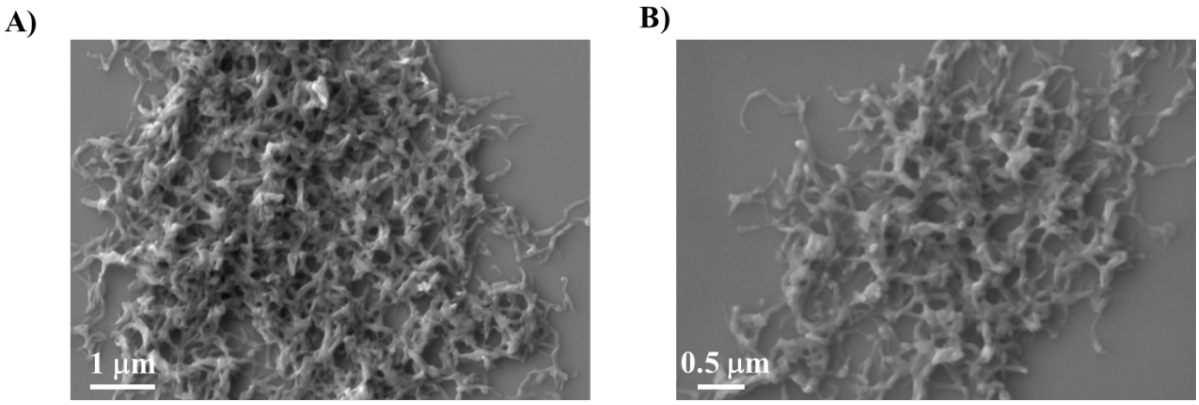

Figure S5. FE-SEM images showing morphology of **Eh-G** aggregated in 10% water in dioxane solution

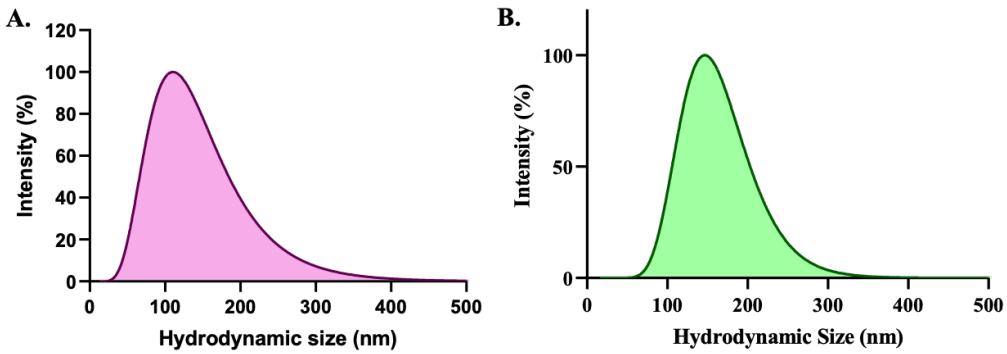

Figure S6. Size analysis by DLS **A.** Size of plain liposome and **B.** Liposome coated **Eh-G** (**L-Eh-G**).

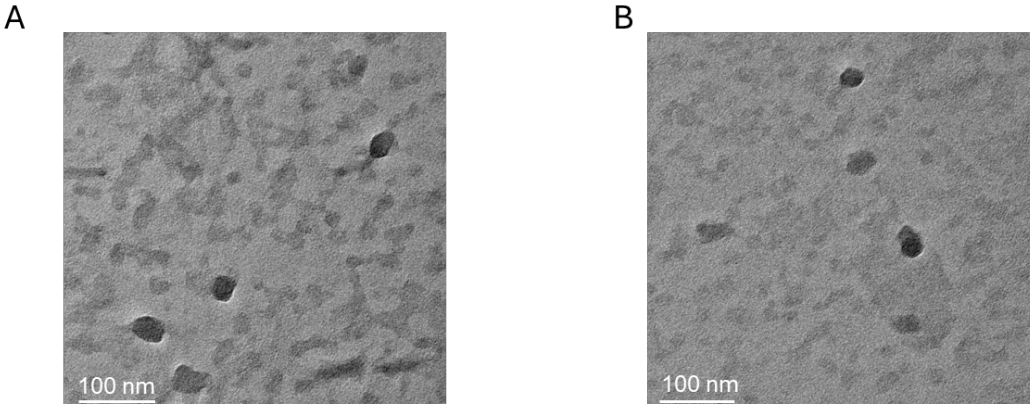

Figure S7. A and **B.** TEM images of liposomes before encapsulating **Eh-G**.

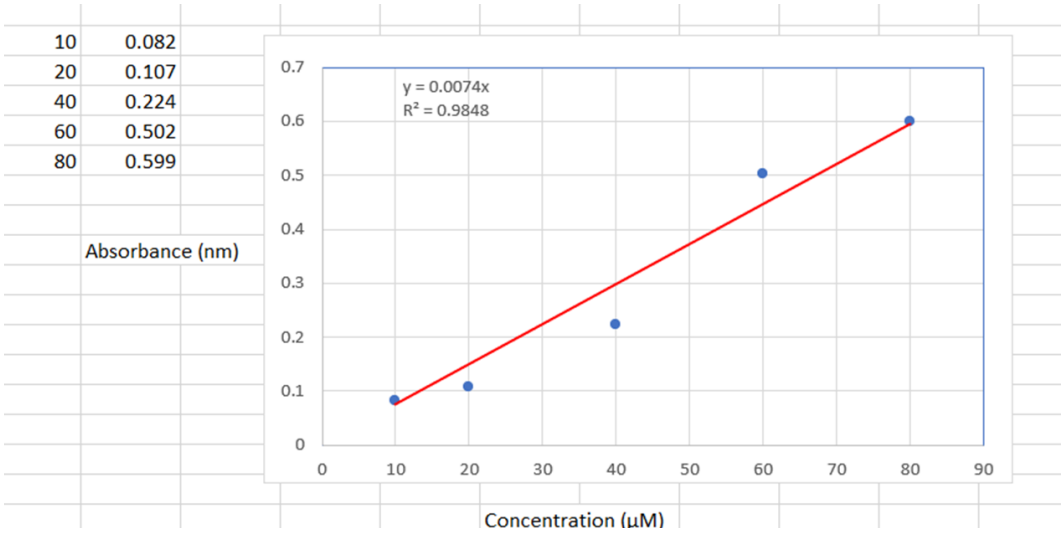

Figure S8. Encapsulation efficiency of **Eh-G** calculated as 73.64%.

Cycles/ 10 mins	Temp. of Control (water)	Liposome	Temp. of L-Eh-G
1st	25.7	27.6	46.7
2nd	24.6	24.8	46.7
3rd	26.5	24.0	46.4
4th	26.3	25.1	46.3
5th	27.7	25.4	46.2

Table S1. Thermal stability with on/off cycles, with each cycle of 10 minutes using a 750 nm laser.

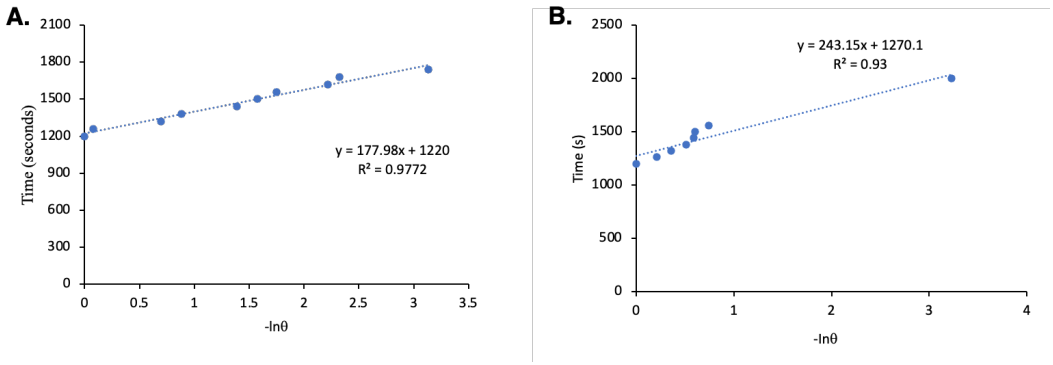

Figure S9. Cooling time as a function of -Ln(θ): **A.** Water and **B. L-Eh-G** sample under 750 nm laser irradiation.

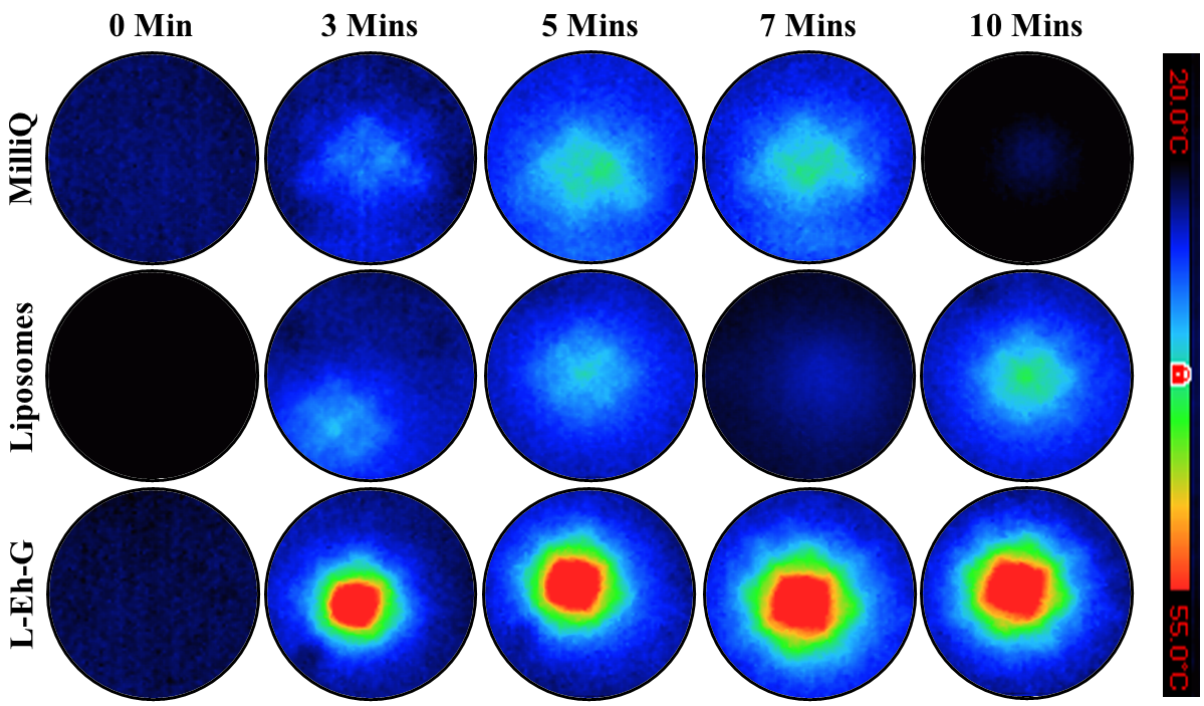

Figure S10. Photothermal transduction efficiency of **L-Eh-G** when irradiated with 808 nm laser.

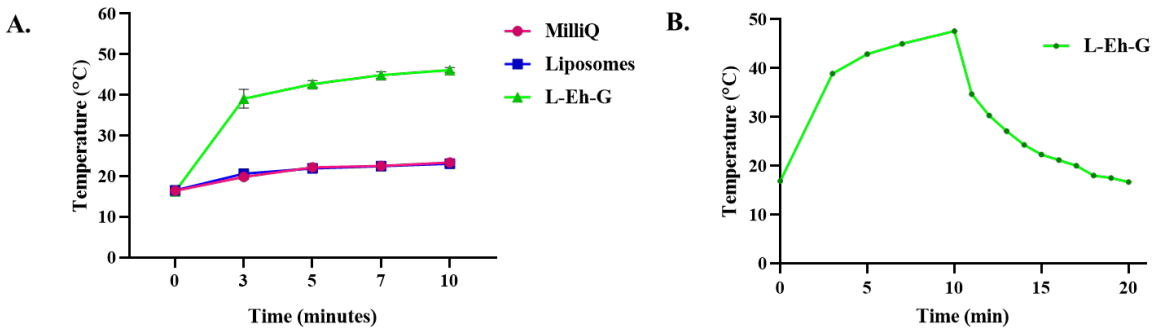

Figure S11. A. Photothermal heating curves of control (Millipore water), free liposome and liposome encapsulated **L-Eh-G** under 808 nm laser **B.** The heating and cooling curves of **L-Eh-G**.

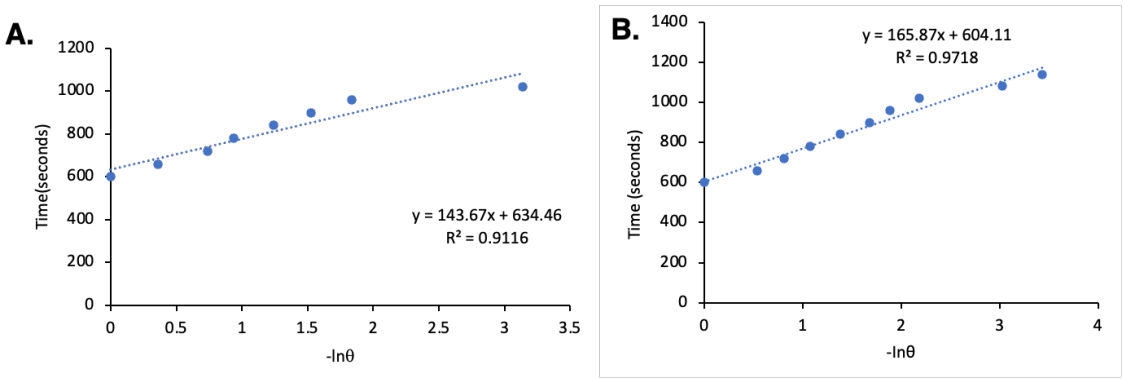

Figure S12. Cooling time as a function of -Ln(θ): **A.** Water and **B. L-Eh-G** sample under 808 nm laser irradiation.

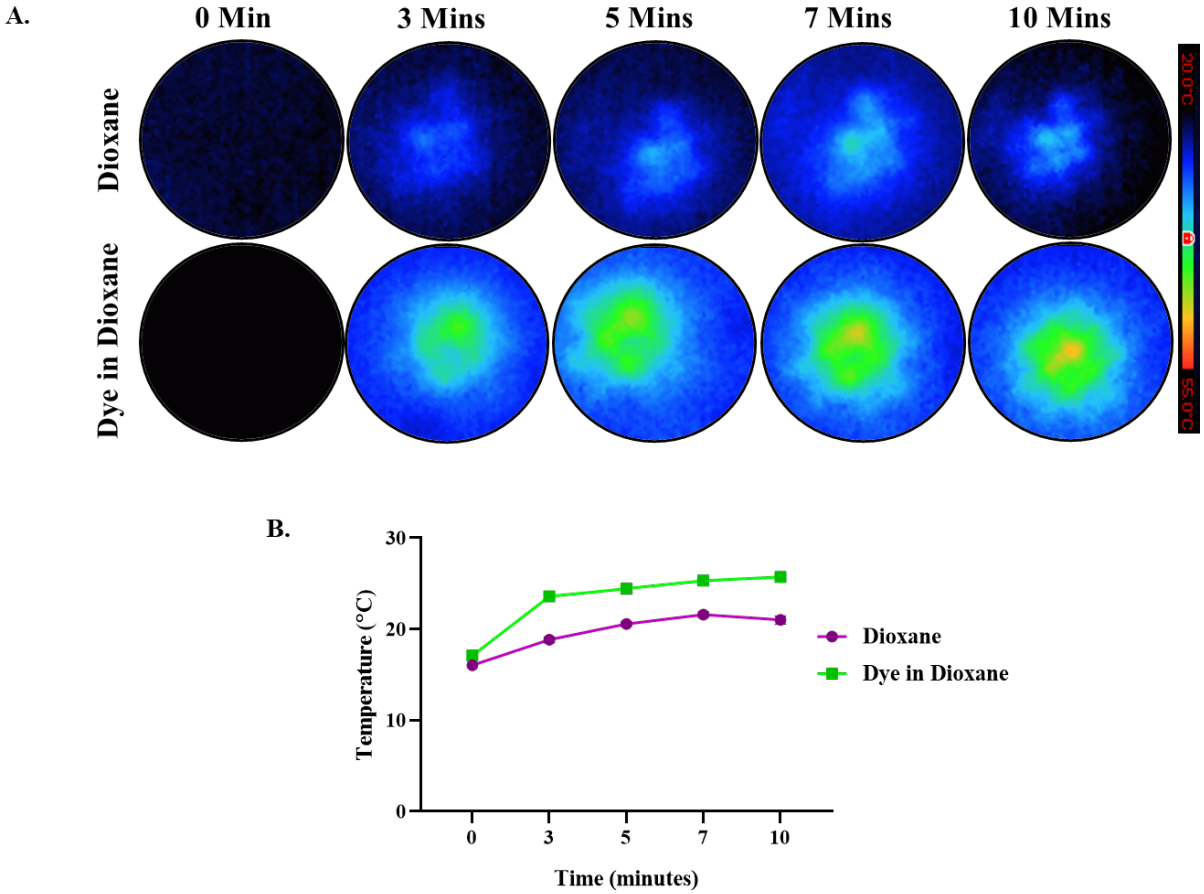

Figure S13. A. Photothermal images of temperature rise when **Eh-G** is taken in dioxane, **B**. Photothermal heating curves of **Eh-G** in dioxane.

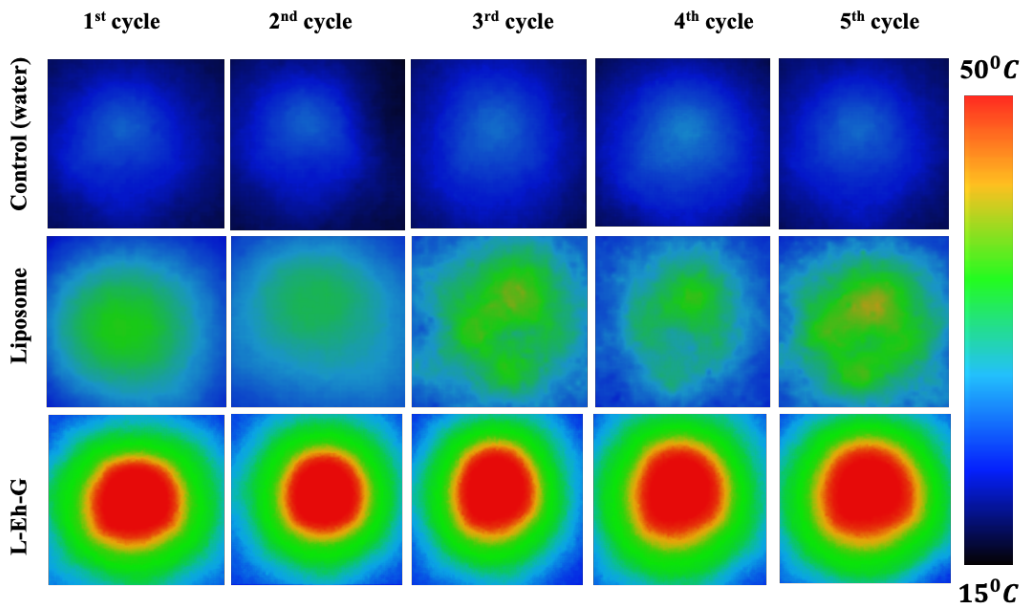

Figure S14. Thermal images for the thermal stability (on/ off cycle) after irradiation with a 750 nm laser of the control (water), **Eh-G** compounds for 10 min (five cycles) without liposomal coating, **L-Eh-G**.

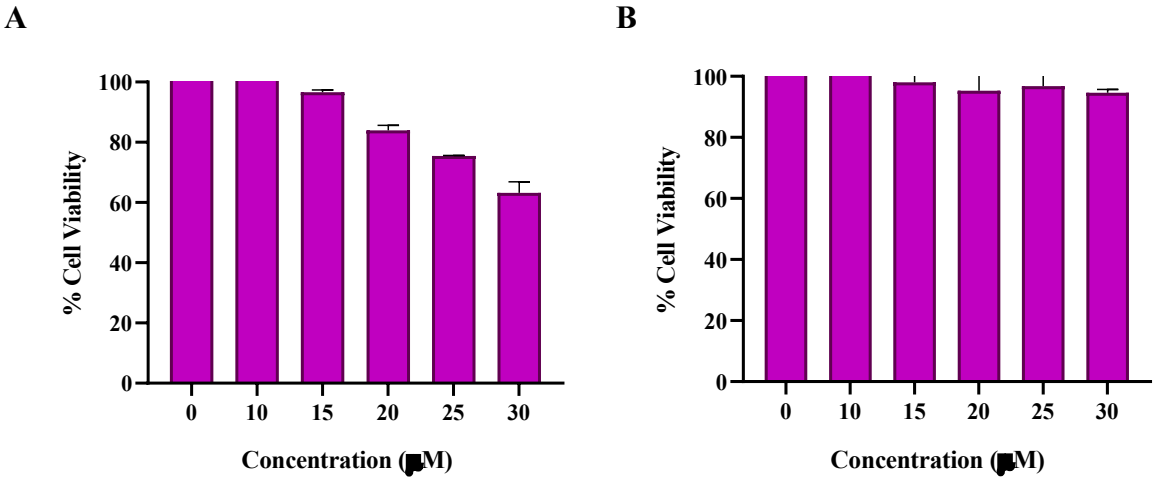

Figure S15. Biocompatibility studies of **A. Eh-G** and **B. L-Eh-G** on NIH 3T3 (mouse embryonic fibroblast cell lines).

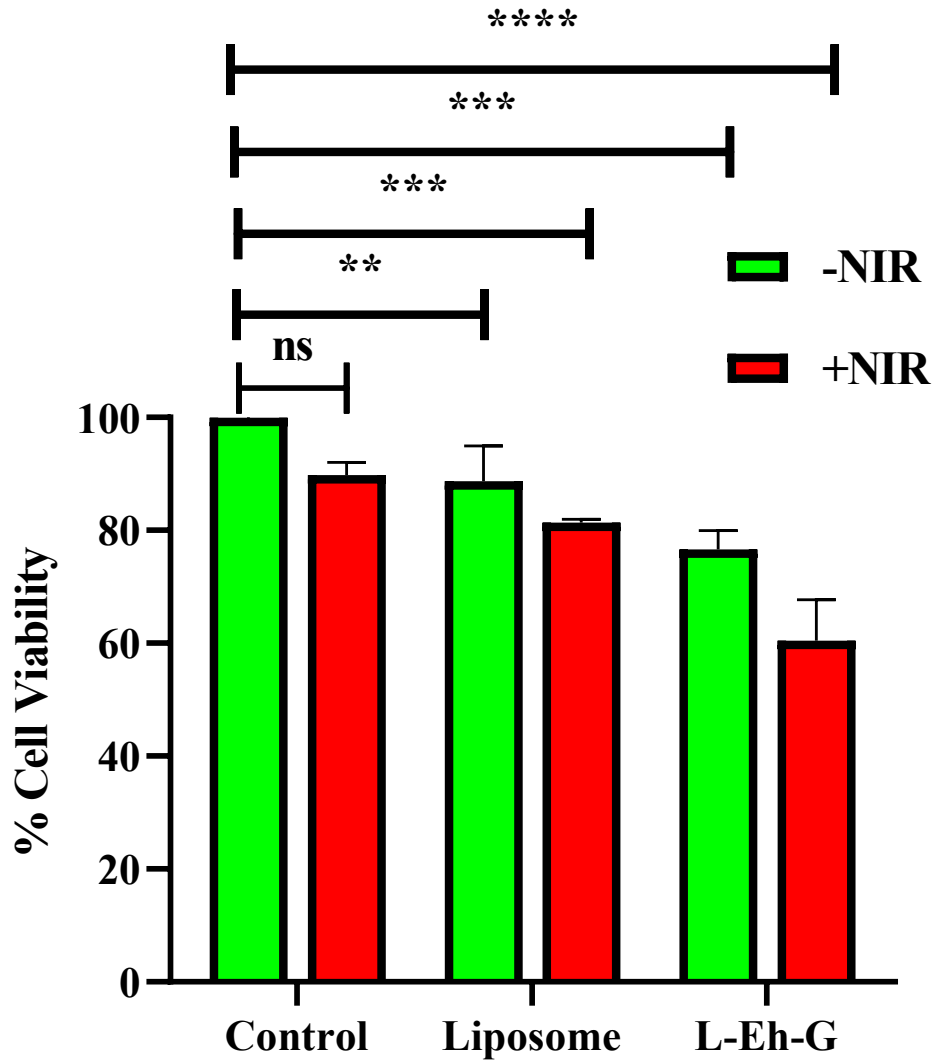

Figure S16. MTT assay- NIR laser mediated cell cytotoxicity of free liposome, **L-Eh-G** (10 μM) in 4T1 cell line, NIR laser irradiation 808 nm.

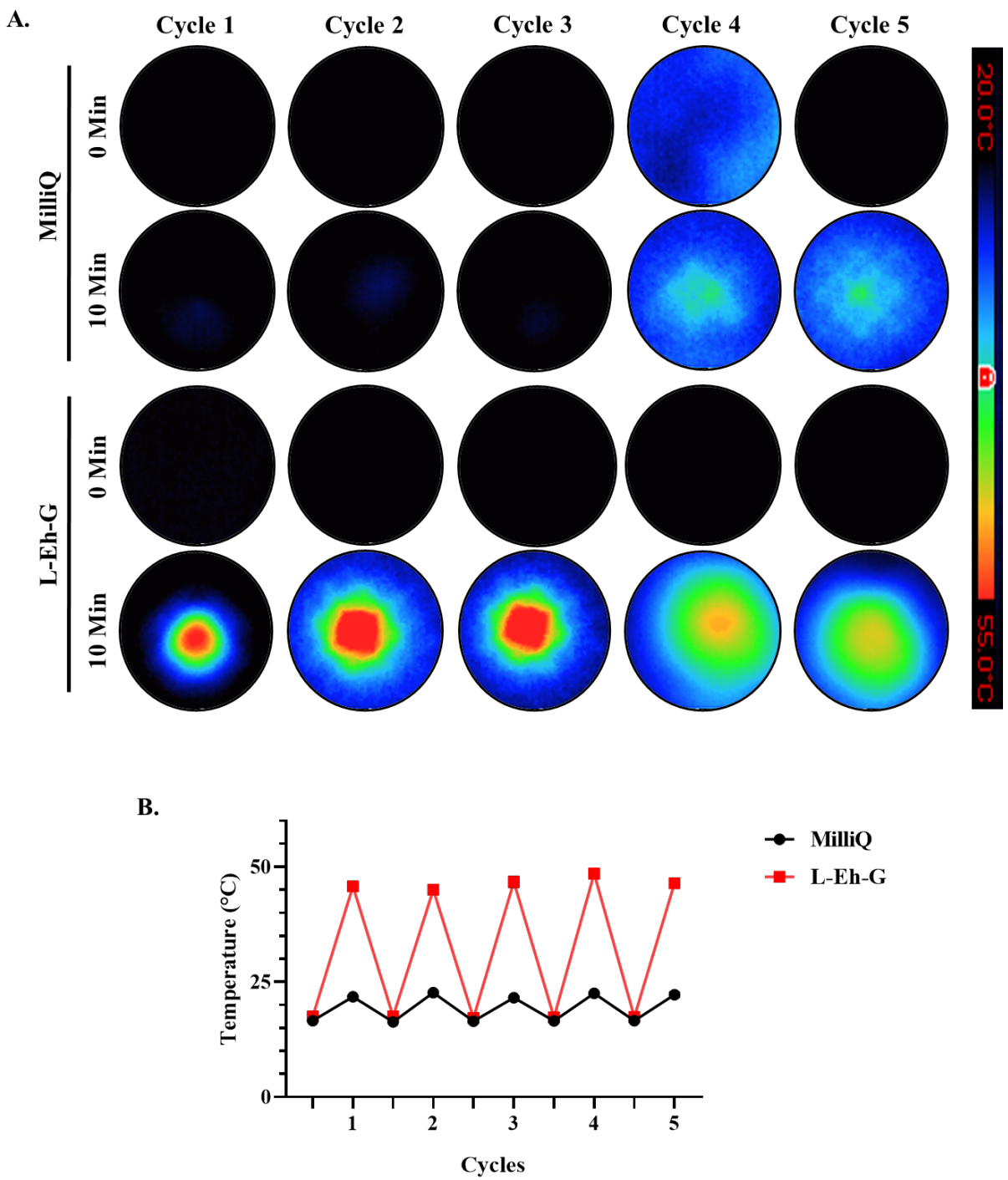

Figure S17. A. Photothermal images of temperature rise in **L-Eh-G** when irradiated with 808 nm laser over 5 heating and cooling cycles. **B**. Graphical representation of thermal stability (on/off cycle) of MilliQ water, free liposome and **L-Eh-G**, after irradiation with a 808 nm (808 mW) laser for 10 minute

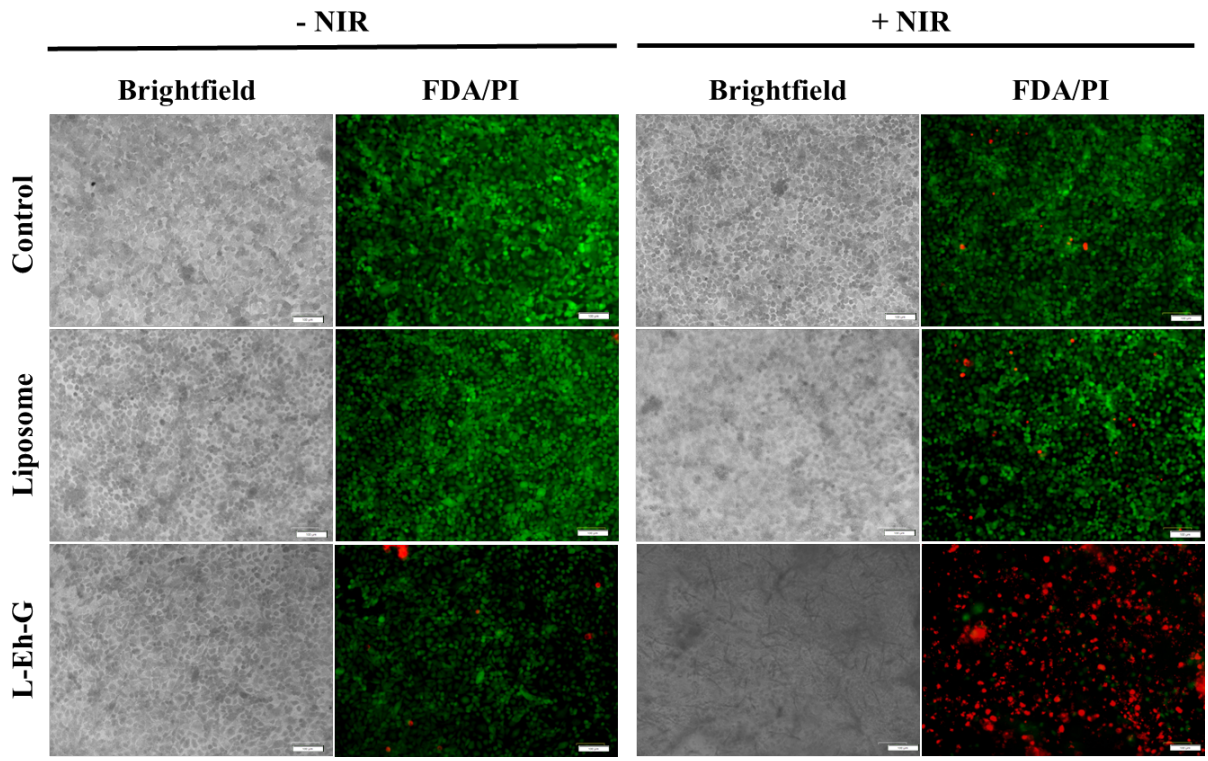

Figure S18. Live-Dead assay for NIR laser mediated cell cytotoxicity of plane liposome, Control and **L-Eh-G** (scale bar: 20 μm). (NIR Laser 808 nm).

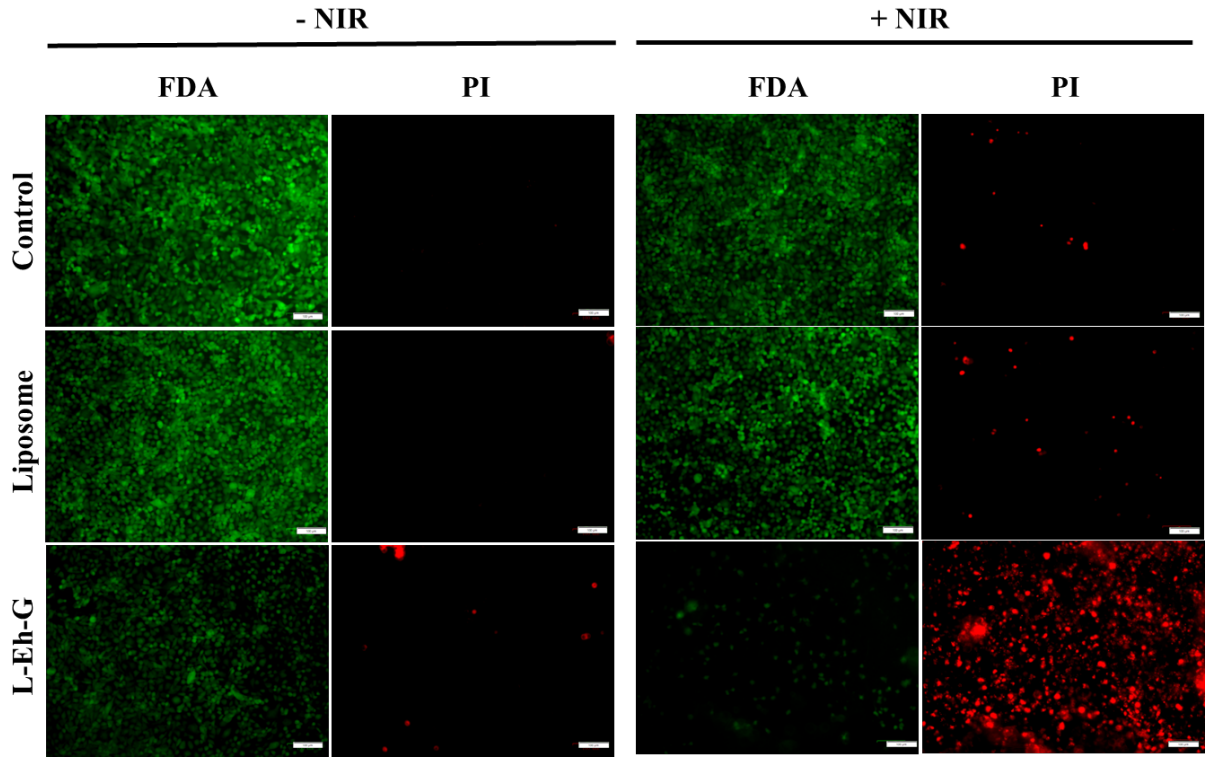

Figure S19. Live-Dead assay for NIR laser mediated cell cytotoxicity of plane liposome, Control and **L-Eh-G** (scale bar: 20 μm). (NIR Laser 808 nm).

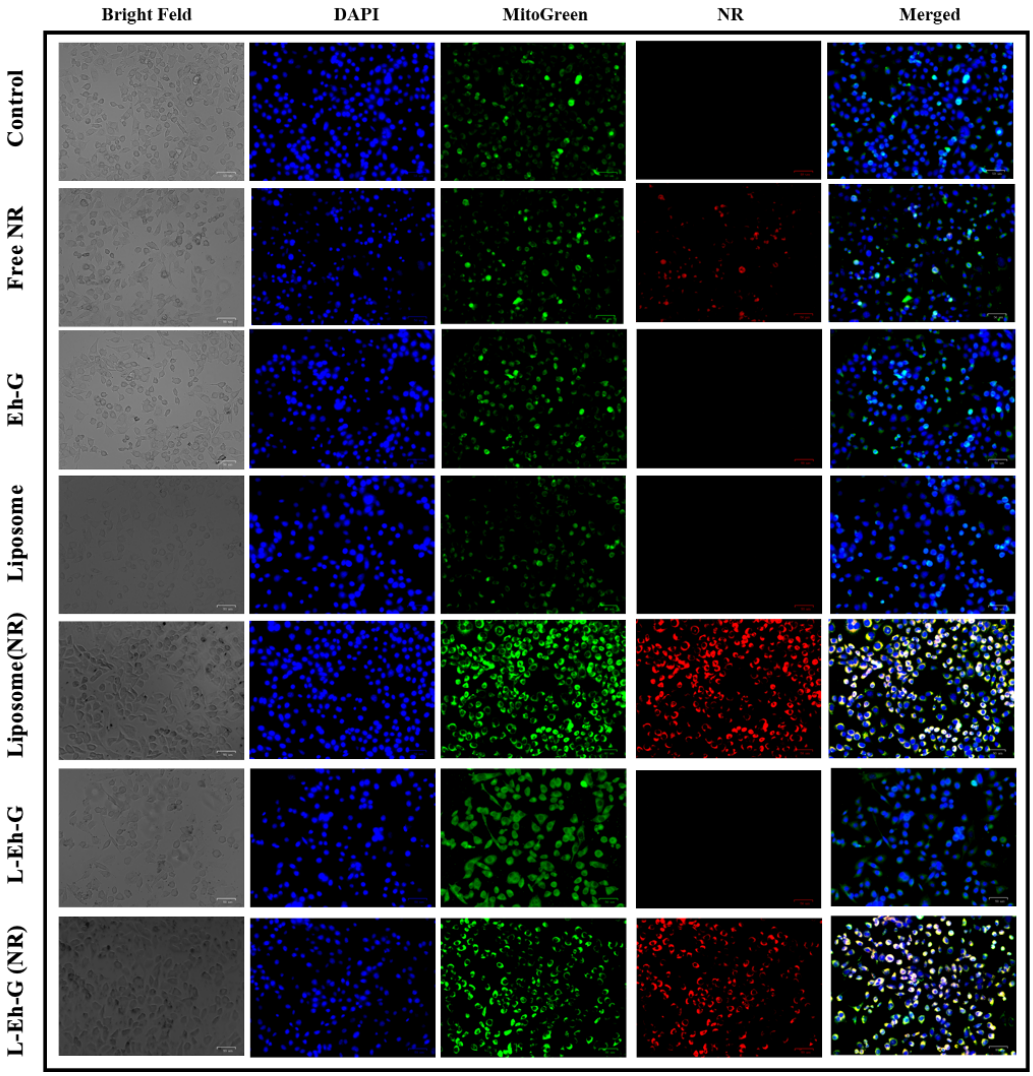

Figure S20. Intracellular uptake studies in 4T1 cells using Fluorescence Microscopy images incubated with **L-Eh-G** (scale bar 50 µm), DAPI (blue) stain nuclei region, MitoGreen (green) stain mitochondria, and NR (red) stain exhibited by NPs tracking in the cytoplasm. Merged images for green and red channels showed co-localization.

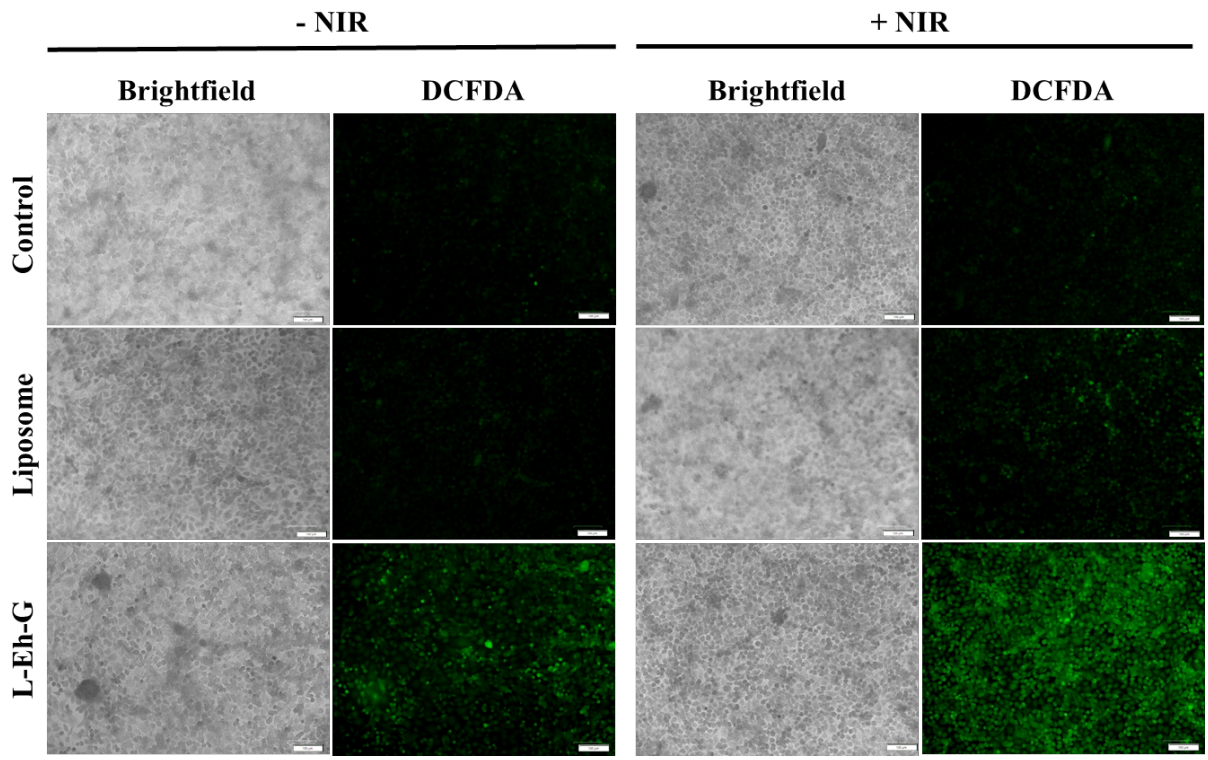

Figure S21. DCFDA analysis after NIR Laser irradiation of Control (water), free liposome, **Eh-G** and **L-Eh-G** for singlet oxygen species production before and after inducing 808 nm NIR laser, scale bar 20 µm. (ex- 485 nm and em- 535 nm).

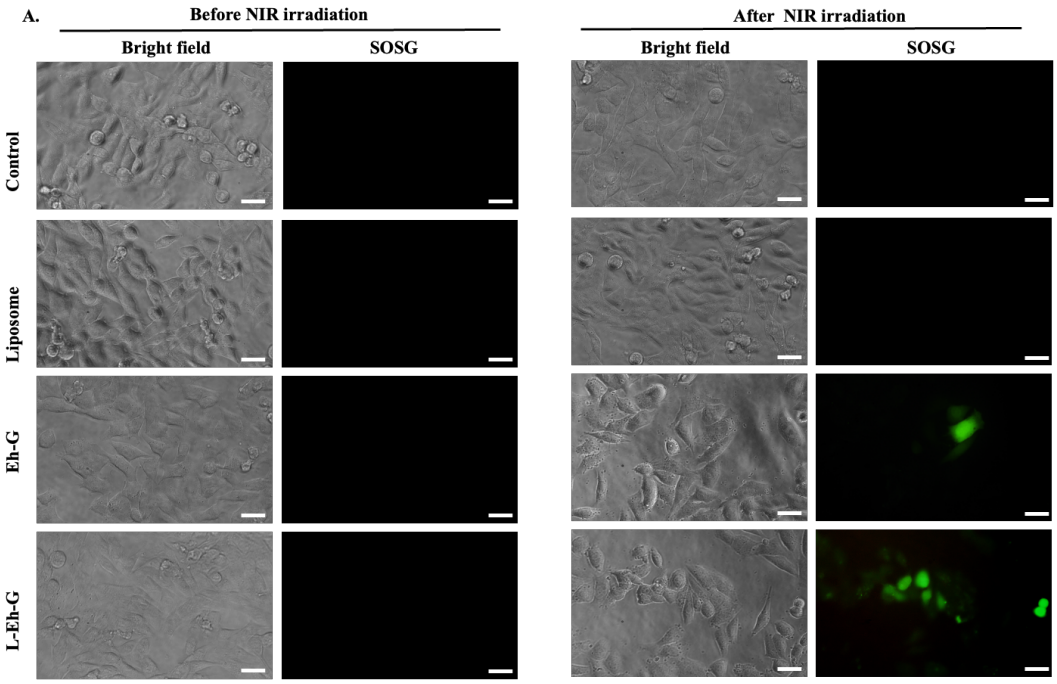

Figure S22. Data for intracellular generation of singlet oxygen species by using SOS G (scale bar, 20 μm) in the A) absence of NIR-laser and B) presence of NIR laser (750 nm).

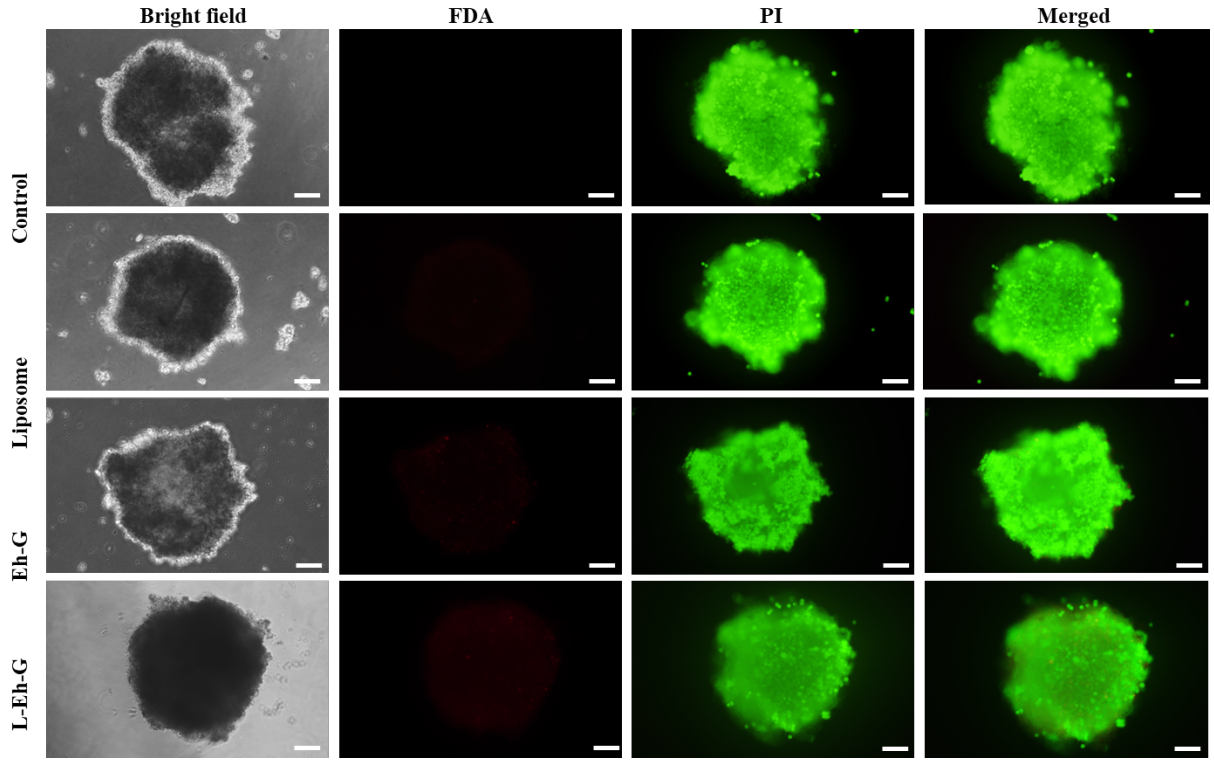

Figure S23. *In vitro* cell cytotoxicity of control water, Free liposome, **Eh-G** and **L-Eh-G** by the live/dead assay (FDA/PI) in a 4T1 3D tumor spheroids cell culture model (scale bar, 100 μm) without NIR-laser (750 nm). Green channel (excitation at 510 nm and emission at 550 nm), Red channel (excitation at 575 nm and emission at 625 nm).

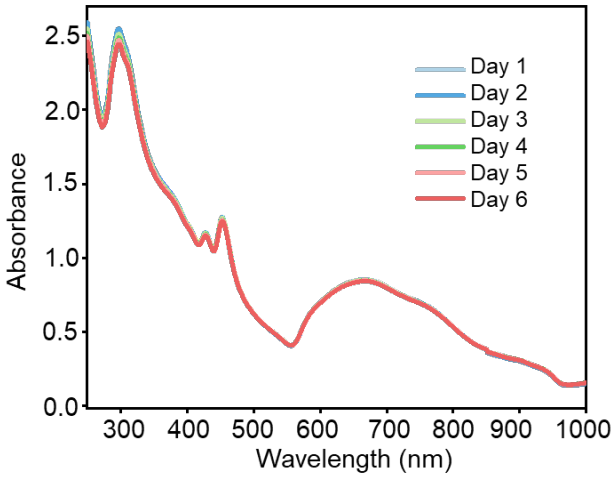

Figure S24. UV-Vis-NIR absorption spectra of **L-Eh-G** in RPMI media recorded for 6 days, indicating its stability in serum containing media.

References

(1) S. Kotha, R. Sahu, D. Srideep, S.S. R. K. C. Yamijala, S. K. Reddy and K. V. Rao, *Chem. Asian J.* 2022, **16**, e202200494.

(2) R. Gayathri, P. S. Rajalakshmi, A. Thomas and A. K. Rengan, *Materialia,* 2021, **19,** 101195.

(3) P. S. Rajalkshmi, B. S. Alvi, N. Begum, B. Veeresh and A. K. Rengan, *Biomacromolecules,* 2021*,* **9***,* 3926-3940.

(4) T. Appidi, D. B. Pemmaraju, R. A. Khan, S. B. Alvi, R. Srivastava, M. Pal, N. Khan and A. K. Rengan, *Nanoscale*, 2020, **12**, 2028–2039

(5) T. appidi, P. S. Rajalkshmi, S. A. Chinchulkar, A. Pradhan, H. Begum, V. Shetty, R. Srivastava, P. Ganesan and A. K. Rengan *Nanoscale*, 2022, **14**, 9112-9123,

(6) S. C. Brüningk, I. Rivens, C. Box, U. Oelfke and G. Haar, *Sci. Rep.,* 2020, **10**, 1653

(7) G. Perini, A. Rosenkranz, G. Friggeri, D. Zambrano, E. Rosa and A. Augello, V. Palmieri, M. D. Spirito, M. Papi, *Biomed. Pharmacother.*, 2022, **153**, 113496.

(8) D. Srideep, S. Khatun, A. K. Rengan and K. V. Rao, *ChemBioChem,* 2023, **8,** e202300007.